Journal of Alloys and Compounds 908 (2022) 164697

Contents lists available at ScienceDirect

Journal of Alloys and Compounds

journal homepage: www.elsevier.com/locate/jalcom

Manipulation of magnetic configuration by isotropic pressure in $NdFeO_3$

Yiming Cao[a,b,*], Yanru Kang[a,b], Jiawang Zhao[a,b], Qi Cui[c,d], Jinguang Cheng[c,d], Xunqing Yin[e], Hongwei Liu[a,b], Yuanlei Zhang[a,b], Xijia He[a,b], Mian Liu[a,b], Shengxian Wei[a,b], Shixun Cao[f], Zhe Li[a,b], Kun Xu[a,b,*]

[a] Center for Magnetic Materials and Devices, College of Physics and Electronic Engineering, Qujing Normal University, Qujing 655011, China
[b] Key Laboratory for Advanced Functional and Low Dimensional Materials of Yunnan Higher Education Institute, Qujing Normal University, Qujing 655011, China
[c] Beijing National Laboratory for Condensed Matter Physics and Institute of Physics, Chinese Academy of Sciences, Beijing 100190, China
[d] School of Physical Sciences, University of Chinese Academy of Sciences, Beijing 100190, China
[e] Institute of Applied Physics and Materials Engineering, University of Macau, Avenida da Universidade, Taipa 999078, Macao Special Administrative Region of China
[f] Department of Physics, International Center of Quantum and Molecular Structures, and Materials Genome Institute, Shanghai University, Shanghai 200444, China

ARTICLE INFO

Article history:
Received 27 April 2021
Received in revised form 4 August 2021
Accepted 21 March 2022
Available online 24 March 2022

Keywords:
Rare-earth orthoferrites
Spin reorientation
Isotropic pressure

ABSTRACT

The influence of isotropic physical pressure, applied either during the high-pressure-high-temperature (HPHT) annealing or the measuring processes, on the magnetic properties of $NdFeO_3$ single crystal, has been investigated. In comparison to the complete spin reorientation (SR) in an as-grown $NdFeO_3$ single crystal, the thermomagnetic $M(T)$ and isothermal $M(H)$ curves for a HPHT-annealed sample indicates an incomplete SR transition from a Γ_2-rich to a Γ_4-rich Γ_{24} mixed phase. Moreover, the $M(T)$ curves of the as-grown sample under different measuring hydrostatic pressures suggest that the SR transition takes place in the sequence of $\Gamma_2 \rightarrow \Gamma_1 + \Gamma_2 + \Gamma_4 \rightarrow \Gamma_1 + \Gamma_4 \rightarrow \Gamma_4$, instead of the $\Gamma_2 \rightarrow \Gamma_2 + \Gamma_4 \rightarrow \Gamma_4$, without applying pressure during the measuring process. Such manipulation of the magnetic configuration reveals that the 3*d*-4*f* interaction in the $NdFeO_3$ could be greatly affected by the isotropic pressure. These findings may provide a new perspective and possibility for the tuning of the magnetism and corresponding microscopic interactions.

1. Introduction

Tailoring magnetic properties by in-situ methods is highly valuable from both the fundamental and practical points of view. Among them, the most common approaches to manipulate magnetization are using magnetic fields [1] or temperature [2]. However, there are still intensive efforts to increase the flexibility and offer additional degrees of freedom in tuning the magnetism via electric fields [3], lasers [4], and uniaxial pressure [5], etc.

In the rare-earth orthoferrites $RFeO_3$ (R = rare earth elements), R^{3+} ions are paramagnetic above its Néel temperature T_{N1} (generally <10 K), whereas Fe^{3+} ions order magnetically below another Néel temperature T_{N2} = 620–740 K with three possible spin configurations: the Γ_1 (A_x, G_y, C_z), Γ_2 (F_x, C_y, G_z) and Γ_4 (G_x, A_y, F_z). Here, the G, C and A following Bertaut's notation [6] refer to different antiferromagnetic (AFM) arrangements of Fe^{3+} ions, whereas the F is the net moment induced by the canted AFM [7]. The subscripts x, y and z represent the ordered magnetic moments along a-, b- and c-axis, respectively. The arrangements of Fe^{3+} moments in the phases of Γ_1, Γ_2 and Γ_4 are sketched in Fig. 1. The magnetic properties of $RFeO_3$ are peculiar due to the complex magnetic interactions (Fe^{3+}-Fe^{3+}, Fe^{3+}-R^{3+} and R^{3+}-R^{3+}), and the competition of these interactions gives rise to various interesting phenomena in these materials. One of outstanding phenomena is the so-called spin reorientation (SR) transition of the Fe^{3+} moments induced by temperature or magnetic field. The observed temperature-induced SR transition in $RFeO_3$ can be classified into two categories as the temperature decreases. The first category is from the Γ_4 to the Γ_2 state, during which the magnetic easy axis direction varies from the c- to the a-axis. The typical representatives are $NdFeO_3$ [8], $SmFeO_3$ [9], $TbFeO_3$ [10], $HoFeO_3$ [11], $ErFeO_3$ [12] and $TmFeO_3$ [4]. The second category is observed in $DyFeO_3$ [13] and $CeFeO_3$ [14]. The corresponding SR transition is from the Γ_4 state to the Γ_1 state, during which the weak ferromagnetism (FM) vanishes and the moments of Fe^{3+} transform into an AFM arrangement.

* Corresponding authors at: Center for Magnetic Materials and Devices, College of Physics and Electronic Engineering, Qujing Normal University, Qujing 655011, China.
E-mail addresses: ymcao@mail.qjnu.edu.cn (Y. Cao), xukun@mail.qjnu.edu.cn (K. Xu).

https://doi.org/10.1016/j.jallcom.2022.164697
0925-8388/

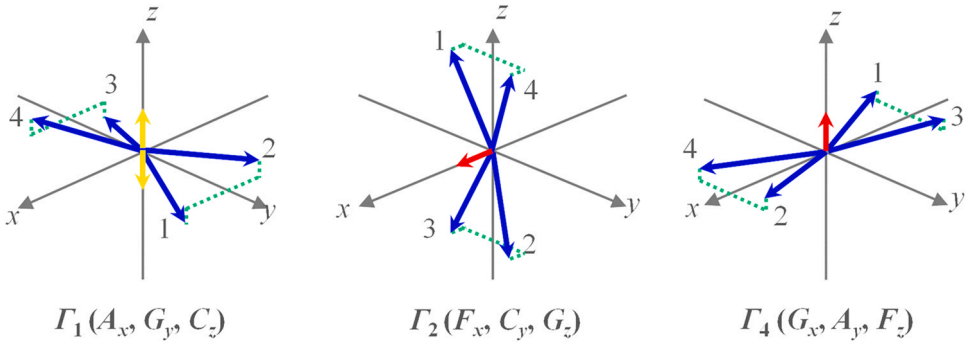

Fig. 1. Sketch of spin arrangements of Fe^{3+} ions in the Γ_1, Γ_2 and Γ_4 phases. Arrows indicate Fe^{3+} moments (blue), superpositions of two diagonal Fe^{3+} moments (yellow) and net moments in a unit cell (red).

As one of the representative rare-earth orthoferrites, $NdFeO_3$ crystallizes in an orthorhombic perovskite structure (space group *Pbnm*). Its SR transition has been extensively investigated by both static and dynamic techniques. Magnetization measurements were used to determine the SR temperature range (macroscopic magnetic properties of the SR transition) [8], and the neutron powder diffraction technique was further implemented to estimate microscopic anisotropy parameters [15]. Moreover, terahertz time domain spectroscopy [16], and the pulse laser pump probe technique [17], have been employed to detect the ultrafast dynamics of spins, electrons, and lattice during the SR transition in $NdFeO_3$. The control of the spin or SR transition by the aforementioned technologies was realized by tuning the lattice parameters or acting on the spins directly.

Based on the anti-symmetric Dzyaloshinsky-Moriya (DM) exchange model [18] and density functional theory, the magneto-crystalline anisotropy of $NdFeO_3$ is determined not only by the Fe-3*d* spin structure, but also by the well-localized Nd-4*f* electrons. Thus, the strong exchange interaction between the Fe-3*d* and the Nd-4*f* magnetic sublattices results in the SR transition. Both magnetic states before and after such transition can be determined by the DM interaction. It is known that the magnetic field and temperature can manipulate the interaction by altering the bond lengths of Fe^{3+}-O^{2-} and R^{3+}-O^{2-}, as well as the bond angles of Fe^{3+}-O^{2-}-Fe^{3+}, Fe^{3+}-O^{2-}-R^{3+} and R^{3+}-O^{2-}-R^{3+}. Thus, applying static isotropic pressure is supposed to be an effective technique to tune these interactions. Two methods are available for the application of static isotropic pressure. One is annealing the single crystal under high-pressure-high-temperature (HPHT) conditions. The other is applying hydrostatic pressure during the magnetic measuring process.

To date, how the structures and magnetism are affected by the hydrostatic pressure have been predicted theoretically [19]. Corresponding experimental research on $TmFeO_3$ has also been reported in our previous work [20]. In this work, we conducted a comparative analysis of the influence of isotropic pressure on the SR transition in both the annealing process and the measuring condition for the $NdFeO_3$ single crystal.

2. Experimental details

Rare-earth orthoferrite $NdFeO_3$ single crystals were grown by an optical floating zone furnace following the procedure described in our previous work [20]. A Rigaku Ultima IV X-ray diffraction (XRD) using Cu-K_α radiation was used to characterize the crystal structure. The crystallographic orientations were identified by Laue X-ray photography (beam diameter of 0.5 mm). The magnetization measurements were acquired using a Quantum Design Versalab system equipped with a Cu–Be clamp-type pressure cell which possesses a maximum pressure of 1.30 GPa. The HPHT annealing of $NdFeO_3$ single crystals was performed with a Kawai-type multi-anvil module (Max Voggenreiter GmbH) in the Institute of Physics, Chinese Academy of Sciences. The as-grown $NdFeO_3$ single crystal specimen was inserted into a hexagonal boron nitride sleeve, and a semi-sintered MgO ceramic octahedron was used as the pressure-transmitting medium. The pressure and temperature implemented in the HTHP annealing process were 7 GPa and 1200 °C, respectively.

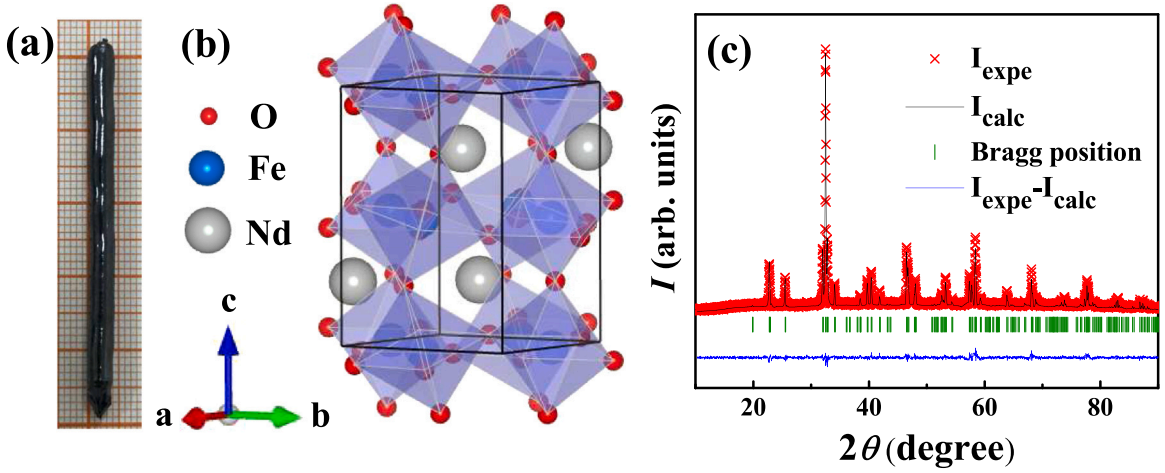

Fig. 2. **(a)** Photograph and **(b)** crystalline structure of $NdFeO_3$ single crystal. **(c)** Rietveld refinement of the powder XRD pattern of crushed $NdFeO_3$ powders.

Table 1
Refined structural parameters with *Pbnm* space group symmetry for $NdFeO_3$ single crystal at room temperature.

Cell parameters				
a (Å)	*b* (Å)	*c* (Å)		
5.4480(2)	5.5840(3)	7.7579(3)		
Reliability Factors				
R_p		R_{wp}	R_{exp}	χ^2
3.01		3.82	3.18	1.45
Atom	*x*	*y*	*z*	*B* (Å^2)
Nd1	-0.0117(6)	0.0507(2)	0.25	1.90(6)
Fe1	0.5	0	0	1.51(10)
O1	0.094(2)	0.491(2)	0.25	0.59(24)
O2	0.714(2)	0.292(2)	0.037(2)	1.21(24)

3. Results and discussion

A black shiny $NdFeO_3$ single crystal of about 4 mm in diameter and 50 mm in length was successfully grown, as shown in Fig. 2(a). For the purpose of determining its crystal structure with high precision, a high-quality Rietveld refinement of room temperature powder XRD data was performed by using the Fullprof software [21], and the refined crystal structure and pattern are displayed in Fig. 2(b) and (c). No traces of impurity phases were detected within the resolution of the XRD. All the peaks observed in the XRD spectra can be well assigned to the orthorhombic structure of space group *Pbnm*. Corresponding refinement results are listed in Table 1.

Fig. 3(a) shows the temperature dependences of magnetization at ambient pressure along the *a*- ($M_a(T)$) and the *c*-axes ($M_c(T)$), in

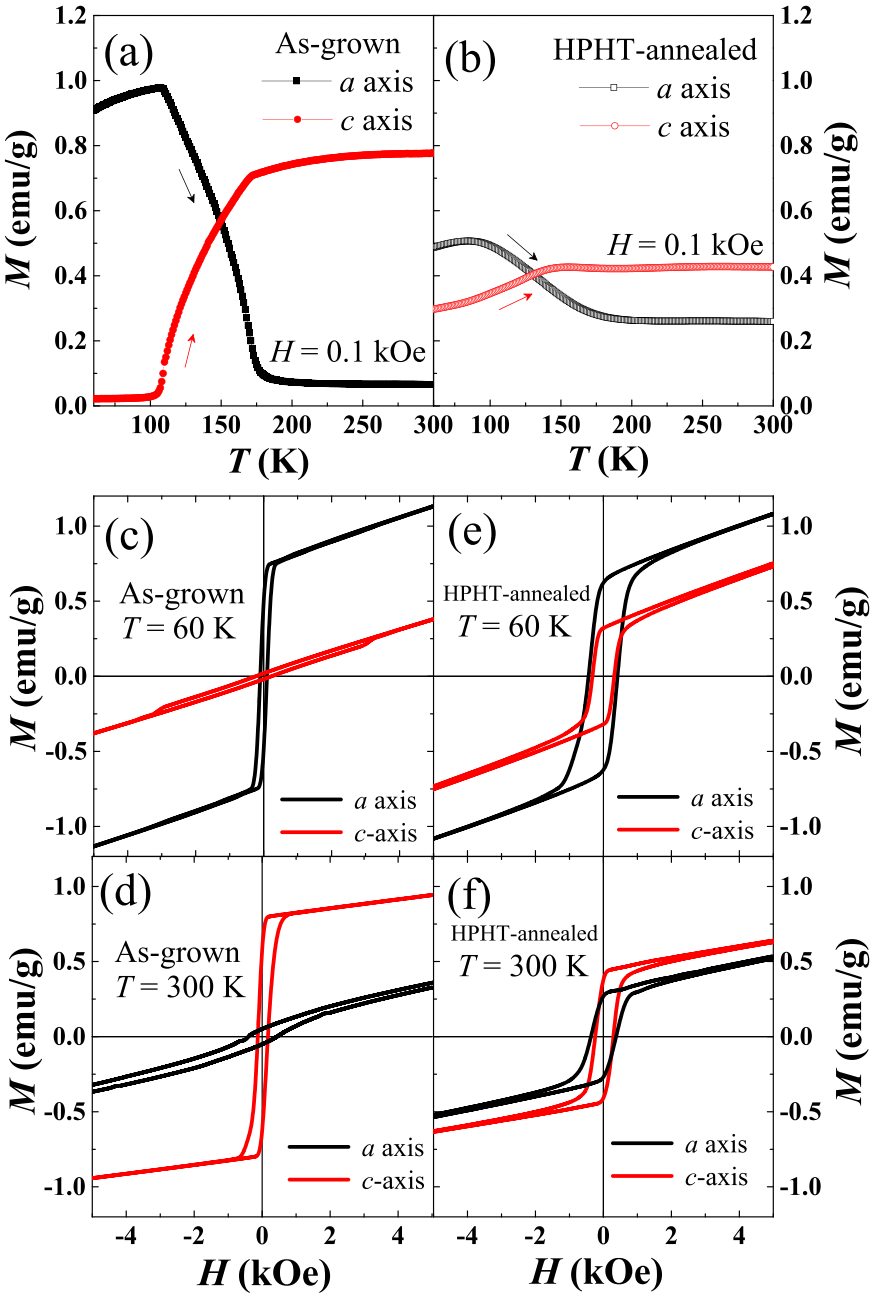

Fig. 3. The $M(T)$ curves of **(a)** the as-grown and **(b)** the HPHT-annealed $NdFeO_3$ single crystal in a magnetic field of 1 kOe. The $M(H)$ curves at 60 K and 300 K for.**(c)-(d)** the as-grown and **(e)-(f)** the HPHT-annealed $NdFeO_3$ single crystal.

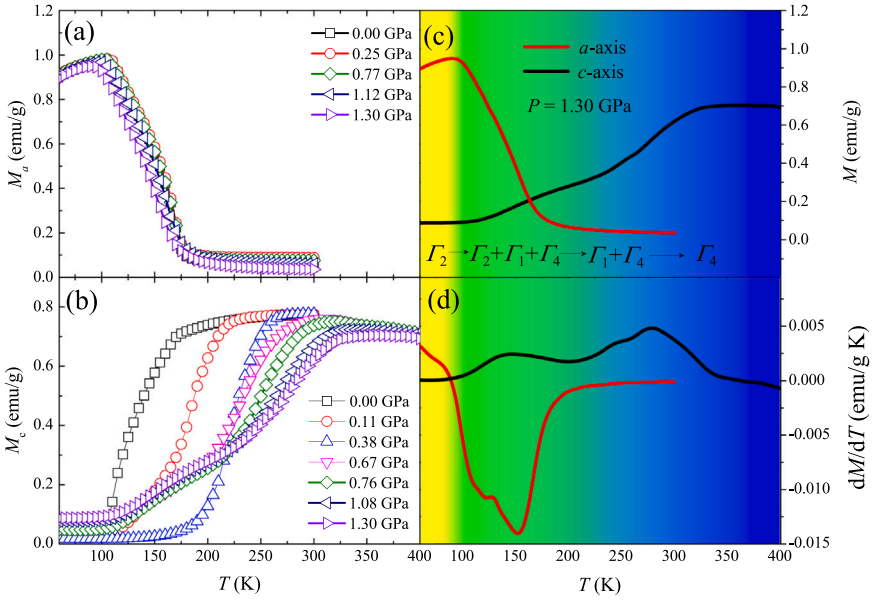

Fig. 4. The **(a)** $M_a(T)$ and **(b)** $M_c(T)$ curves under different hydrostatic pressures, **(c)** $M(T)$ and **(d)** dM/dT curves at 1.30 GPa as an example, for the as-grown $NdFeO_3$ single crystal. The yellow, green, light blue, and dark blue regions represent the Γ_2, $\Gamma_1+\Gamma_2+\Gamma_4$, $\Gamma_1+\Gamma_4$ and Γ_4 states, respectively.

field-cooled-warming (FCW) mode with a 0.1 kOe magnetic field, for the as-grown $NdFeO_3$ single crystal. It is found that the $M_a(T)$ drops between ~100 and ~180 K, and the $Mc(T)$ jumps up in the same temperature range. They cross each other at ~149 K. Such an orientation phase transition is attributed to a SR transition from Γ_2 to Γ_4 with the help of an intermediate phase Γ_{24}, with a continuous rotation of the weak FM moment from the a to the c axis. To study the influence of isotropic physical pressure on the SR transition during the sample preparation process, the $M_a(T)$ and $M_c(T)$ curves of the HPHT-annealed $NdFeO_3$ single crystal were also measured under the same conditions as the as-grown one. As shown in Fig. 3(b), similar trends in $M_a(T)$ and $M_c(T)$ curves of the HPHT-annealed $NdFeO_3$ crystal are observed with those of the as-grown crystal. Nevertheless, the changes in magnetization are much weaker (ΔM_a ~ 0.23 emu/g and ΔM_c ~ 0.13 emu/g) for the HTHP annealed sample compared to those (ΔM_a ~ 0.89 emu/g and ΔM_c ~ 0.68 emu/g) of the as-grown one, indicating an incomplete transition from a Γ_2-rich to a Γ_4-rich Γ_{24} mixed phase. The overall effect is the continuous rotation of the weak FM vector by a certain acute angle θ, rather than 90°, in the ac-plane.

To verify the above hypothesis, the magnetization curves of $M_a(H)$ and $M_c(H)$ were measured for the as-grown and HPHT-annealed crystals. For the as-grown sample, the $M_a(H)$ at 300 K and $M_c(H)$ at 60 K revealed a weak FM character with obvious coercivity of ~100 Oe, whereas the $M_c(H)$ at 300 K and $M_a(H)$ at 60 K presented a linear magnetic field dependence corresponding to the AFM state, as shown in Fig. 3(c) and (d), in accordance with the behavior of $\Gamma_2 \rightarrow \Gamma_4$ SR transition. However, for the HPHT-annealed sample, as shown in Fig. 3(e) and (f), all the $M_a(H)$ and $M_c(H)$ curves at 60 K and 300 K exhibited the FM behavior with larger coercivities of 300–400 Oe, confirming the fact that the transition occurs between mixed phases of Γ_2 and Γ_4. The partial orientation phase transition and larger coercivity in the HPHT-annealing condition are probably because the HPHT annealing process forms dislocations/defects and magnetic domains, and thus the rotation of spin is constrained to some extent. The formation of the magnetic domain mainly comes from the existence of dislocations/defects as the grain boundaries induced by the HPHT-annealing.

The effect of external hydrostatic pressure on the SR transition during the measuring process has also been evaluated. Fig. 4(a) and (b) show the $M_a(T)$ and $M_c(T)$ curves of the as-grown sample in a field of 0.1 kOe under different hydrostatic pressures up to 1.30 GPa. It was found that the SR transition in $M_a(T)$ is almost unaffected by the application of hydrostatic pressure, indicating no significant changes in length in the a axis during SR, which is in a good agreement with Ref. 15. In contrast, in the c axis, the SR transition shifts to significantly higher temperatures due to the hydrostatic pressure, and its final temperature reaches over 300 K under an external pressure of 1.30 GPa. Such a shift with pressure contradicts the fact that no abrupt changes in lattice parameter c [15], revealing the complexity of the influence of pressure on the exchange interaction between the Fe-3d and the Nd-4f magnetic sublattices. By a careful inspection, only the SR transition under the pressures < 0.38 GPa transforms directly from the Γ_2 to the Γ_4 state. Once the hydrostatic pressure exceeds 0.67 GPa, the transition is markedly widened and proceeds in multiple stages. As an example, the $M_a(T)$ and $M_c(T)$ curves at 1.30 GPa, and their corresponding differential dM/dT curves, are replotted in Fig. 4(c) and (d). As presented in Fig. 4(d), two anomalies (just one single anomaly) can be observed in the dM_c/dT (dM_a/dT) curve, where the low-temperature peak in dM_c/dT approximately parallels the main anomaly in dM_a/dT over the temperature range 90–200 K, whereas the high-temperature anomaly in dM_c/dT remains in the range of 200–360 K. By combining dM/dT with the $M(T)$ data in Fig. 4(c), such a transition during warming can be divided into multiple stages as follows: (i) In the region ~60 < T < ~90 K, the sample is in the pure Γ_2 state. (ii) In the region ~90 < T < ~200 K, the M_a decrease indicates the reduction of the Γ_2 phase, and the slight increase of M_c reveals the appearance of Γ_4. However, the small magnitudes of both M_a and M_c infer the existence of the intermediate phase Γ_1. Thus, this temperature region should be attributed to the mixed phases of Γ_1, Γ_2 and Γ_4. (iii) In the region ~200 < T < ~340 K, the M_a drops to zero, suggesting the disappearance of the Γ_2 phase, and thus the existence of only the Γ_1 and Γ_4 phases. (iv) With further warming to above ~340 K, the sample transforms completely to the pure Γ_4 state. Therefore, it can be concluded that the transition takes place in the sequence of $\Gamma_2 \rightarrow \Gamma_1+\Gamma_2+\Gamma_4 \rightarrow \Gamma_1+\Gamma_4 \rightarrow \Gamma_4$. The presence of such an intermediate phase Γ_1 during the $\Gamma_2 \rightarrow \Gamma_4$ SR transition under hydrostatic pressure was also observed in $TmFeO_3$ single crystals.

The comparative studies for the influence of the static isotropic pressure, either applied during the annealing process or the measuring condition, on the SR transition have been conducted. We can

conclude that both these two different types of isotropic pressure can affect the magnetic configuration, as well as the 3*d*-4*f* interaction, in $NdFeO_3$.

4. Conclusion

In summary, we have successively grown the $NdFeO_3$ single crystal with a single-phase perovskite structure by the optical floating zone method. Both the $M(T)$ and $M(H)$ curves for the HPHT-annealed sample indicate an incomplete transition from a Γ_2-rich to a Γ_4-rich Γ_{24} mixed phase. Furthermore, the $M(T)$ curves of the as-grown sample under different hydrostatic pressures suggest that the SR transition in $NdFeO_3$ takes place in the sequence of $\Gamma_2 \rightarrow \Gamma_1 + \Gamma_2 + \Gamma_4 \rightarrow \Gamma_1 + \Gamma_4 \rightarrow \Gamma_4$. Such comparative studies on the influence of isotropic pressure on SR transition suggest that the magnetic configuration and the 3*d*-4*f* coupling in $NdFeO_3$ could be modified by both types of isotropic pressures.

CRediT authorship contribution statement

Yiming Cao: Conceptualization, Formal analysis. **Yanru Kang**: Data curation, Formal analysis. **Jiawang Zhao**: Methodology. **Qi Cui**: Methodology. **Jinguang Cheng:** Methodology. **Xunqing Yin**: Software. **Hongwei Liu**: Data Curation, Methodology. **Yuanlei Zhang**: Data Curation, Methodology. **Xijia He**: Visualization. **Mian Liu**: Writing-review & editing. **Shengxian Wei**: Investigation, Writing-review & editing. **Shixun Cao**: Supervision. **Zhe Li**: Supervision, Writing-review & editing. **Kun Xu**: Conceptualization, Funding acquisition, Writing-original draft, Writing-review & editing.

Declaration of Competing Interest

The authors declare that they have no known competing financial interests or personal relationships that could have appeared to influence the work reported in this paper.

Acknowledgments

This work is supported by the National Natural Science Foundation of China (NSFC, Nos. 51862032, 51861032, 11774217, 12064035, 12025408, 11874400), the Project for Applied Basic Research Programs of Yunnan Province (Nos. 2018FA031, 2018FB010), the Yunnan Local Colleges Applied Basic Research Projects of Yunnan Province (Nos. 2018FH001-001, 2017FH001-047), and Program for Innovative Research Team (in Science and Technology) in University of Yunnan Province (IRTSTYN).

Conflicts of interest

The authors declare no conflict of interest.

References

[1] J. Nogués, I.K. Schuller, Exchange bias, J. Magn. Magn. Mater. 192 (1999) 203–232.
[2] N. Hur, S. Park, P. Sharma, J. Ahn, S. Guha, S. Cheong, Electric polarization reversal and memory in a multiferroic material induced by magnetic fields, Nature 429 (2004) 392–395.
[3] H. Ohno, D. Chiba, F. Matsukura, T. Omiya, E. Abe, T. Dietl, Y. Ohno, K. Ohtani, Electric-field control of ferromagnetism, Nature 408 (2000) 944–946.
[4] A. Kimel, A. Kirilyuk, A. Tsvetkov, R. Pisarev, T. Rasing, Laser-induced ultrafast spin reorientation in the antiferromagnet $TmFeO_3$, Nature 429 (2004) 850–853.
[5] S. Ikeda, N. Shirakawa, T. Yanagisawa, Y. Yoshida, S. Koikegami, S. Koike, M. Kosaka, Y. Uwatoko, Uniaxial-pressure induced ferromagnetism of enhanced paramagnetic $Sr_3Ru_2O_7$, J. Phys. Soc. Jpn. 73 (2004) 1322–1325.
[6] E.F. Bertaut, 4 - Spin Configurations of Ionic Structures: Theory and Practice, in: G.T. Rado, H. Suhl (Eds.), Spin Arrangements and Crystal Structure, Domains, and Micromagnetics, Academic Press, 1963, pp. 149–209.
[7] R.L. White, Review of recent work on the magnetic and spectroscopic properties of the rare-earth orthoferrites, J. Appl. Phys. 40 (1969) 1061–1069.
[8] S.J. Yuan, W. Ren, F. Hong, Y.B. Wang, J.C. Zhang, L. Bellaiche, S.X. Cao, G. Cao, Spin switching and magnetization reversal in single-crystal $NdFeO_3$, Phys. Rev. B 87 (2013) 184405.
[9] J.-H. Lee, Y.K. Jeong, J.H. Park, M.-A. Oak, H.M. Jang, J.Y. Son, J.F. Scott, Spin-canting-induced improper ferroelectricity and spontaneous magnetization reversal in $SmFeO_3$, Phys. Rev. Lett. 107 (2011) 117201.
[10] Y. Cao, M. Xiang, W. Zhao, G. Wang, Z. Feng, B. Kang, A. Stroppa, J. Zhang, W. Ren, S. Cao, Magnetic phase transition and giant anisotropic magnetic entropy change in $TbFeO_3$ single crystal, J. Appl. Phys. 119 (2016) 063904.
[11] X. Zeng, X. Fu, D. Wang, X. Xi, J. Zhou, B. Li, Terahertz time domain spectroscopic investigation of spin reorientation transitions in $HoFeO_3$, Opt. Express 23 (2015) 31956–31963.
[12] H. Shen, Z. Cheng, F. Hong, J. Xu, S. Yuan, S. Cao, X. Wang, Magnetic field induced discontinuous spin reorientation in $ErFeO_3$ single crystal, Appl. Phys. Lett. 103 (2013) 192404.
[13] Y. Tokunaga, S. Iguchi, T. Arima, Y. Tokura, Magnetic-field-induced ferroelectric state in $DyFeO_3$, Phys. Rev. Lett. 101 (2008) 097205.
[14] S.J. Yuan, Y.M. Cao, L. Li, T.F. Qi, S.X. Cao, J.C. Zhang, L.E. DeLong, G. Cao, First-order spin reorientation transition and specific-heat anomaly in $CeFeO_3$, J. Appl. Phys. 114 (2013) 113909.
[15] W. Sławiński, R. Przeniosło, I. Sosnowska, E. Suard, Spin reorientation and structural changes in $NdFeO_3$, J. Phys. Condens. Matter 17 (2005) 4605–4614.
[16] J. Jiang, Z. Jin, G. Song, X. Lin, G. Ma, S. Cao, Dynamical spin reorientation transition in $NdFeO_3$ single crystal observed with polarized terahertz time domain spectroscopy, Appl. Phys. Lett. 103 (2013) 062403.
[17] R.V. Mikhaylovskiy, E. Hendry, V.V. Kruglyak, R.V. Pisarev, T. Rasing, A.V. Kimel, Terahertz emission spectroscopy of laser-induced spin dynamics in $TmFeO_3$ and $ErFeO_3$ orthoferrites, Phys. Rev. B 90 (2014) 184405.
[18] I. Dzyaloshinsky, A thermodynamic theory of "weak" ferromagnetism of antiferromagnetics, J. Phys. Chem. Solids 4 (1958) 241–255.
[19] H.J. Zhao, W. Ren, Y. Yang, X.M. Chen, L. Bellaiche, Effect of chemical and hydrostatic pressures on structural and magnetic properties of rare-earth orthoferrites: a first-principles study, J. Phys. Condens. Matter 25 (2013) 466002.
[20] Y. Cao, Q. Zhuang, S. Wei, X. Yin, H. Liu, Y. Zhang, Y. Kang, X. He, M. Liu, S. Cao, Y. Yang, Z. Li, K. Xu, Evidence of magneto-structural coupling during the spin reorientation process in $TmFeO_3$ single crystal, J. Magn. Magn. Mater. 523 (2021) 167626.
[21] H.M. Rietveld, A profile refinement method for nuclear and magnetic structures, J. Appl. Crystallogr. 2 (1969) 65–71.